sciendo

Int. J. of Applied Mechanics and Engineering, 2022, vol.27, No.4, pp.26-39
DOI: 10.2478/ijame-2022-0048

STROUHAL NUMBER EFFECTS ON DYNAMIC BOUNDARY LAYER EVOLUTION OVER A WEDGE SURFACE FROM INITIAL FLOW TO STEADY FLOW: ANALYTICAL APPROACH

Mohamed BACHIRI*
Matter Sciences Department, Faculty of Sciences -University of Amar Telidji
B.P 37 G, Laghouat 03000, ALGERIA
E-mail: mabach73@yahoo.fr

Ahcen BOUABDALLAH
Thermodynamics and Energetical Systems Laboratory, Faculty of Physics/USTHB
B.P 32 El Alia, 16111 Bab Ezzouar-Algiers, ALGERIA

The present work studies the effects of the physical parameter characterizing the laminar flow regime, namely the Strouhal number, on the evolution of the unsteady dynamic boundary-layer developed along a wedge surface. Similarity method is used to transform unsteady momentum equation to dimensionless form. Using superposition method between diffusion and convective flows solutions, an ad hoc velocity profile formula is proposed. The obtained results confirm perfectly the numerical data given by Blasius, Falkner-Skan and Williams-Rhyne for all Strouhal numbers. A new accurate analytical function of the local skin friction is established for all time values and for different wedge surface directions. In order to give further clarification on the flows evolutions from diffusion flow to convective flow, in the whole space domain, new skin friction coefficient curves are plotted for all Strouhal numbers and for different wedge surface directions.

Key words: unsteady boundary layer, wedge surface, Strouhal number, superposition method, diffusion, convective.

1. Introduction

Our main objective is to find an analytical approach allowing a solution of nonlinear equations governing the fluid flow, with the aim of applying it to thermal and mass transfers. In addition, the approximate solution of the dynamic boundary layers should be simple and with a maximum of three terms to render to it possible use it in the coupling equations. The literature shows that among many theoretical attempts, the similarity is considered the most suitable transformation to reduce the number of variables in nonlinear differential equations in fluid mechanics. Stewartson [1, 2] studied numerically the unsteady momentum equation of viscous incompressible fluid flows past an impulsively semi-infinite horizontal surface started from rest. The authors outlined the main result, i.e. the independence in time disappears in an exponential. Tokudi [3] investigated fluid flow in a dynamic boundary layer on the plate stretching suddenly from rest. The author showed that the flow evolves from the initial Rayleigh flow to the final Blasius flow and the solution develops in temporal power series. Numerical solutions describe the unsteady laminar thermal boundary layer on a semi-infinite flat plate impulsively moving for several Prandtl numbers. A temperature condition imposed on the wall is taken as a parietal condition, Watkins [4]. Hall and Dennis [5, 6] used a numerical iterative method to solve the unsteady boundary layer equations along an impulsive flat surface. In the study, the velocity profile and shear stress are presented in two flow regimes namely: Rayleigh and Blasius. Seshadri *et al.* [7] studied unsteady mixed convection of a heated vertical wall in impulsive motion of the free flow. They

* To whom correspondence should be addressed

solved numerically the unsteady boundary layer equations of momentum and heat by using the finite difference approach. Williams and Rhyne [8] carried out a study of the unsteady dynamic boundary layer on a wedge subjected to a sudden movement (Falkner-Skan type, $\left(u = Cx^m\right)$. The boundary layer equation is solved numerically by using similarity transformations called Williams-Rhyne transformations. Nazar *et al.* [9] studied the unsteady momentum equation of a suddenly stretched surface in a rotating fluid. Using similarity transformation, perturbation and asymptotic solutions are given for small times and large times, respectively. Other similar problems have been solved numerically by many researchers using the Williams-Rhyne transformation, e.g., the study of the stretching plate for various positions in heat transfer and in the presence of a magnetic field. Liao [10] developed a new analytical approach, a homotopy analysis method (*HAM*), for nonlinear problems. Liao [11] achieved an analytic expression of the friction coefficient valid over a large time interval on a flat plate pulled sharply into its plane from rest. The solved equations are those of the dynamic boundary layer where the Rhyne similarity transformations are adopted. Hang [13-14] used a homotopy analysis method to resolve the dynamic and thermal problems in unsteady boundary layer evolved in an electric fluid flowing on the plate exposed at once to a sudden movement and to a thermal shock. The author illustrated that the serial solution results are accurate. Zheng and Ghate [18] solved the problem of the unsteady boundary layer on a flat plate. They worked out an adequate solution using two parameters, the Blasius parameter and dimensionless time. The authors found closed-form solutions valid for other types of flow. Hafidzuddin *et al.* [19] by using appropriate similarity variables resolved both the dynamic and thermal problems of flow over permeable stretching/shrinking surface. The EDP equations were transformed to ordinary equations. The researchers showed the solution stability. Recently, J. Nagler [20] found a higher-order solution of the boundary layer in terms of velocity profile on cylindrical surface subject to sudden movement. The author found that the velocity profiles are identical to those described in the literature which confirms Watson theory. Bulgakov *et al.* [21] used special coordinates to resolve the equation of movement over a blunt body. The Paulhasen approximation is adopted to find different thicknesses in dynamic and thermal boundary layers. Bachiri and Bouabdallah [16], presented an approximate analytical solution of the unsteady dynamic boundary layer equation over a plate by using ad hoc solution for all values of the Strouhal number. The principal result concerned the evolution of the skin friction coefficient in two regime flows from initial to steady solutions. They also [17] studied the steady state momentum and energy equations over an isothermal wedge surface and gave a new expression of the Nusselt number valid for all Prandtl numbers and for different wedge surface positions. So, as a complementary investigation given in [17], we investigate the unsteady dynamic boundary layer over a wedge surface to establish an analytical formulation of the velocity profile as a function of Strouhal numbers over all time values. In addition, in this paper, an analytical expression of the velocity is proposed by superposition method, which must consider the boundary conditions, the solutions of Rayleigh, Blasius and Falkner-Skan, and the equilibrium of the unsteady momentum equation.

2. Mathematical formulations

The geometry of this phenomenon is illustrated in Fig.1, where an unsteady laminar flow expanded along a wedge surface. The velocity components according to the *x* and *y* coordinates are *u* and *v*, respectively, where *x* is tangent to the wedge surface and *y* is perpendicular to *x*. Along the wedge surface and at any time, the velocity vector is equal to zero (adhesion condition). The volume force and the dissipation terms are neglected, and the fluid flow is assumed incompressible. Hence, the continuity and the unsteady momentum equations are:

$$\frac{\partial u}{\partial x} + \frac{\partial v}{\partial y} = 0, \tag{2.1}$$

$$\frac{\partial u}{\partial t} + u\frac{\partial u}{\partial x} + v\frac{\partial u}{\partial y} = u_e(x)\frac{du_e(x)}{dx} + \nu\frac{\partial^2 u}{\partial y^2} \tag{2.2}$$

where $u_e(x) = u_0 x^m$ is the fluid velocity at infinity, m is the Falkner-Skan parameter given by $m = b/(2-b)$ and u_0 is a constant, v and t are, respectively, the kinematic viscosity and the time. These equations are subject to the following conditions:

$$
\begin{aligned}
&t \geq 0: \\
&u(x,0,t) = v(x,0,t) = 0\,, \\
&u(x, y \to \infty, t) = u_e(x)\,, \\
&t = 0: \\
&u(x,y,0) = v(x,y,0) = 0\,.
\end{aligned}
\tag{2.3}
$$

In order to reduce the number of variables in the momentum equation, it was a question of finding the physical parameter that characterizes the fluid flow, then performing an adequate scale analysis. The scale analysis is based on the dimension order of the boundary layer thicknesses of two limits solutions; initial solution $(t = 0)$ and steady solution $(t \to \infty)$.

It was found that, for the initial solution the scale is $\eta_d = y/(nt)^{1/2}$ where the dimension order of diffusion thickness is $\delta_d \approx 3.64(nt)^{1/2}$, and for the steady solution the scale is $\eta_c = y(u_e/nx)^{1/2}$ where the dimension order of convective boundary layer thickness is equal to $\delta_c \approx 5(nx/u_e)^{1/2}$. The scale analysis permits us to deduce the following dimensionless number: $\frac{\delta_c}{\delta_d} = \sqrt{\frac{x}{u_e t}} = St_x^{1/2}$ where $St_x = \frac{x}{u_e t}$ is the local Strouhal number.

The flow regime characterization can be given by the Strouhal number; for $St_x << 1$ the flow is convective (Falkner-Skan flow), for $St_x >> 1$ the flow is diffusive (Rayleigh flow) (see Fig.1).

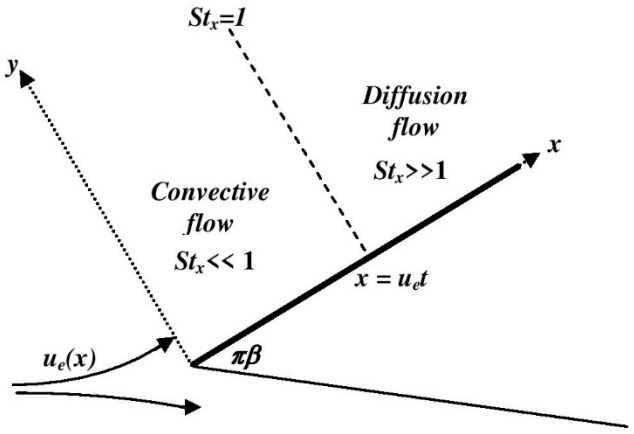

Fig.1. Unsteady flow along a wedge surface.

Thus, the *y*-coordinate scaling is like $y/(nt)^{1/2}$ for a short time $(St_x >> 1)$ and $y(u_e/nx)^{1/2}$ for large times $(St_x << 1)$. The time scale is chosen so that the region of time integration may become finite. Taking into account the previous analysis, the transformations looked for are given by Williams and Rhyne [8]:

$$\eta = y\sqrt{\frac{u_e(x)}{\nu x\xi}},\ \xi = 1-\exp\left(-\frac{u_e t}{x}\right) = 1-\exp\left(-\frac{1}{St_x}\right) \text{ and } \psi(x,y,t) = \sqrt{\nu x\xi u_e(x)}F(\xi,\eta)$$

where η and ξ are the similarity variables, $\psi(x,y,t)$ and $F(\eta,\xi)$ are the streamliness function and the dimensionless stream function, respectively.
Using the similarity transformation and reduced stream function $F(\eta,\xi)$ in Eq.(2.2), the unsteady momentum equation is reduced to

$$\begin{aligned}&\frac{\partial^3 F}{\partial\eta^3}+\frac{1}{2}\eta(1-\xi)\frac{\partial^2 F}{\partial\eta^2}+\frac{1}{2}\left[(m+1)\xi-(m-1)(1-\xi)\ln(1-\xi)\right]F\frac{\partial^2 F}{\partial\eta^2}+\\&-(m-1)\left[\xi(1-\xi)\ln(1-\xi)\frac{\partial F}{\partial\xi}\right]\frac{\partial^2 F}{\partial\eta^2}+m\xi\left[1-\left(\frac{\partial F}{\partial\eta}\right)^2\right]+\\&+\xi(1-\xi)\left[1-(m-1)\ln(1-\xi)\frac{\partial F}{\partial\eta}\right]\frac{\partial}{\partial\xi}\left(\frac{\partial F}{\partial\eta}\right)=0.\end{aligned} \tag{2.4}$$

Subject to boundary conditions: $F(\infty,\xi)=F_\eta(\infty,\xi)=0$ and $F_\eta(\infty,\xi)=1$.

3. Analytical approach

3.1. Case of diffusion flow $(St_x >> 1, \xi = 0)$

When $\xi = 0$, corresponding to $St_x \to \infty$, Eq.(2.4) becomes the Rayleigh type of equation

$$\frac{\partial^3 F}{\partial\eta^3}+\frac{1}{2}\eta\frac{\partial^2 F}{\partial\eta^2}=0 \tag{3.1}$$

subject to: $F(0,0)=0$, $F_\eta(0,0)=0$ and $F_\eta(\infty,0)=1$.
Rayleigh found the exact solution:

$$F_\eta(\eta,0)=erf\left(\frac{\eta}{2}\right) \tag{3.2}$$

where $erf(h)$ is the error function.

3.2. Case of convective flow ($St_x << 1$, $\xi = 1$)

At $\xi = 1$, $(St_x \to 0)$, Eq.(2.4) becomes the Falknar-Skan equation

$$\frac{\partial^3 F}{\partial \eta^3}+\frac{m+1}{2}F\frac{\partial^2 F}{\partial \eta^2}-m\left(\frac{\partial F}{\partial \eta}\right)^2+m=0\,. \tag{3.3}$$

subject to: $F(0,1)=0$, $F_\eta(0,1)=0$ and $F_\eta(\infty,1)=1$.

To our knowledge the exact analytic solution of the non-linear equations such as Eq.(3.3) does not exist. Equation (3.3) admits numerical solutions and analytical approaches with a high order of approximation. In our study given in [17], an accurate analytical approach is proposed using a dimensionless velocity profile formula $F_\eta(\eta,1)$. The choice of $F_\eta(\eta,1)$ expression is constrained to satisfy two fundamental restrictions which are the boundary conditions and the equilibrium of the momentum equation. The proposed dimensionless velocity profile is written as:

$$F_\eta(\eta,1)=-A\exp(-\alpha_0\eta^2)-(B\eta+C)\exp(-\beta_0\eta)+1 \tag{3.4}$$

where A, B, C, α_0 and β_0 are and their determination takes into account the above conditions:

- Boundary conditions give:

$$F_\eta(0,1)=-A-C+1=0\,,$$
$$F_\eta(\eta_\infty,1)=1\,. \tag{3.5}$$

- At $\eta=0$, the Falkner-Skan equation gives:

$$F_{\eta\eta\eta}(0,1)=2A\alpha_0+2B\beta_0-\beta_0{}^2C\,. \tag{3.6}$$

And from the second derivative of Eq.(3.4) at $\eta=0$:

$$F_{\eta\eta}(0,1)=-B+\beta_0 C=cte \tag{3.7}$$

which represents the local shear stress.

$F_{\eta\eta}(0,1)$ and $F_{\eta\eta\eta}(0,1)$ vary according to the wedge surface directions.

From Eq.(3.7): $F_{\eta\eta\eta}(0,1)=-m$ and $F_{\eta\eta}(0,1)$ are given numerically.

At any wedge surface directions, the constants A and C are positives and less than one.

$$A+C=1 \text{ with } 0<A<1 \text{ and } 0<C<1 \tag{3.8}$$

From Eq.(3.7):

$$B=(1-A)\beta_0-F_{\eta\eta}(0,1) \tag{3.9}$$

Equations (3.6)-(3.9) reduce the number of variables like:

$$(1-A)\beta_0{}^2-2F_{\eta\eta}(0,1)\beta_0+(2A\alpha_0+m)=0 \tag{3.10}$$

Because all constants are positives, the solution of this last equation is written as

$$B = (1-A)\beta_0 - F_{\eta\eta}(0,1) = \sqrt{F_{\eta\eta}{}^2(0,1) - (1-A)(2A\alpha_0 + m)}\,, \tag{3.11}$$

$$F_{\eta\eta}^2(0,1) \rangle \sigma(A,\alpha_0) \tag{3.12}$$

where $\sigma(A,\alpha_0) = (1-A)(2A\alpha_0 + m)$.

To find the three constants in Eq.(3.12), the idea is to fix the constant α_0 to a maximum value for all $A \in]\,0,\,1[$ for all wedge surface directions. Figure 2 presents $\sigma(A,\alpha_{0\max})$ and $F_{\eta\eta}^2(0,1)$ according to A for five wedge surface directions. It noticed that $\sigma(A,\alpha_{0\max}) < F_{\eta\eta}^2(0,1)$ with $0 < \alpha_0 \leq \alpha 0_{\max}$.

Thus, the values of $\alpha_{0\max}$ are *0.2203*, *0.4055*, *0.55*, *0.7768* and *1.9095* for *m=0*, *1/9*, *1/5*, *1/3* and *1*, respectively. Using the dichotomous method and Eq.(3.11), it is easy to determine B and β_0 by fixing $\alpha_0 \in]\,0,\,\alpha_{0\max}$ [then selecting the values of $A \in]\,0,\,1[$. The constants in Eq.(3.4) must be justified by the calculation of the residual errors $\Delta\varepsilon$ of Eq.(3.13).

$$\frac{\partial^3 F}{\partial \eta^3} + \frac{m+1}{2} F \frac{\partial^2 F}{\partial \eta^2} - m\left(\frac{\partial F}{\partial \eta}\right)^2 + m = \Delta\varepsilon \tag{3.13}$$

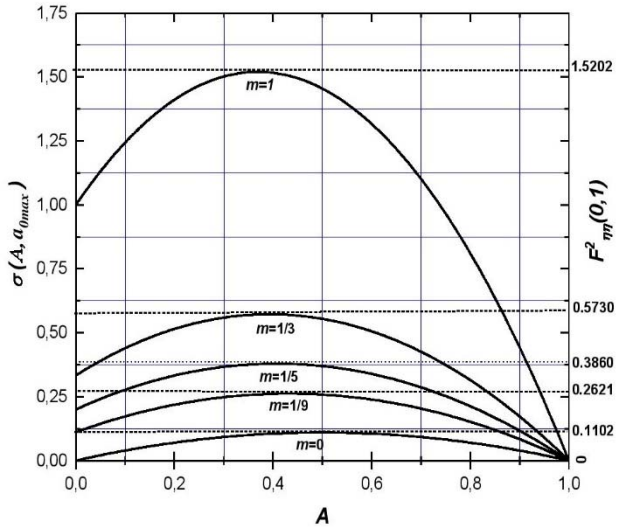

Fig.2. $\sigma(A,\alpha_{0\max})$ and $F_{\eta\eta}^2(0,1)$ variations according to $A \in]0,\,1[$ for five wedge surface directions.

Table 1 gives the values of A, B, C, α_0 and β_0 for five wedge surface directions.

Table 1. Values of constants for different wedge surface directions.

m	***A***	***B***	***C***	α_0	β_0
0	*0.64*	*0.18123*	*0.36*	*0.168*	*1.42581*
1/9	*0.37*	*0.27494*	*0.63*	*0.25*	*1.24913*
1/5	*0.31*	*0.3397*	*0.69*	*0.31*	*1.39275*
1/3	*0.235*	*0.40938*	*0.765*	*0.42*	*1.52520*
1	*0.132*	*0.65849*	*0.865*	*0.95*	*2.17867*

As shown in Fig.3, the results attained denote that Eq.(3.13) converges in the whole spacial domain $0 \le \eta < \infty$ to the solution $F_\eta(\eta, 1)$ of Eq.(3.4) and the mean residual error $\varepsilon < 0.003$ in the whole spacial domain. Indeed, the present analytic approach coincides completely with the numerical results of Blasius and Falkner-Skan for the horizontal and vertical wedge surface.
Thus, we can easily deduce analytically all functions appearing in the momentum equation such as :

$$F(\eta, 1) = -\frac{A\sqrt{\pi}}{2\sqrt{\alpha_0}} erf\left(\sqrt{\alpha_0}\eta\right) + \left[\frac{B}{\beta_0}\eta + \left(\frac{B}{\beta_0^2} + \frac{C}{\beta_0}\right)\right]\exp(-\beta_0\eta) + \eta - \left(\frac{B}{\beta_0^2} + \frac{C}{\beta_0}\right), \tag{3.14}$$

$$F_{\eta\eta}(\eta, 1) = 2A\alpha_0\eta\exp(-\alpha_0\eta^2) + (B\beta_0\eta + C\beta_0 - B)\exp(-\beta_0\eta), \tag{3.15}$$

$$F_{\eta\eta\eta}(\eta, 1) = (-4A\alpha_0^2\eta^2 + 2A\alpha_0)\exp(-\alpha_0\eta^2) + (-B\beta_0^2\eta - C\beta_0^2 + 2B\beta_0)\exp(-\beta_0\eta). \tag{3.19}$$

Figures 4-5 illustrate the stream function and the velocity profiles for five wedge surface directions. It is found that when the wedge angle increases the velocity profiles become narrower because in the dynamic boundary layer the velocity gradient from the wedge surface to the ambient free flow is more rapid when the wedge angle increases. The graphical presentation of Eqs.(3.15)-(3.19), for five wedge surface directions, is given in Figs 6-7, respectively. The main observation from these figures is the competitiveness between convective and diffusion forces, especially near the wall, in which $F_{\eta\eta}(0, 1)$ and $F_{\eta\eta\eta}(0, 1)$ increase when *m* increases.

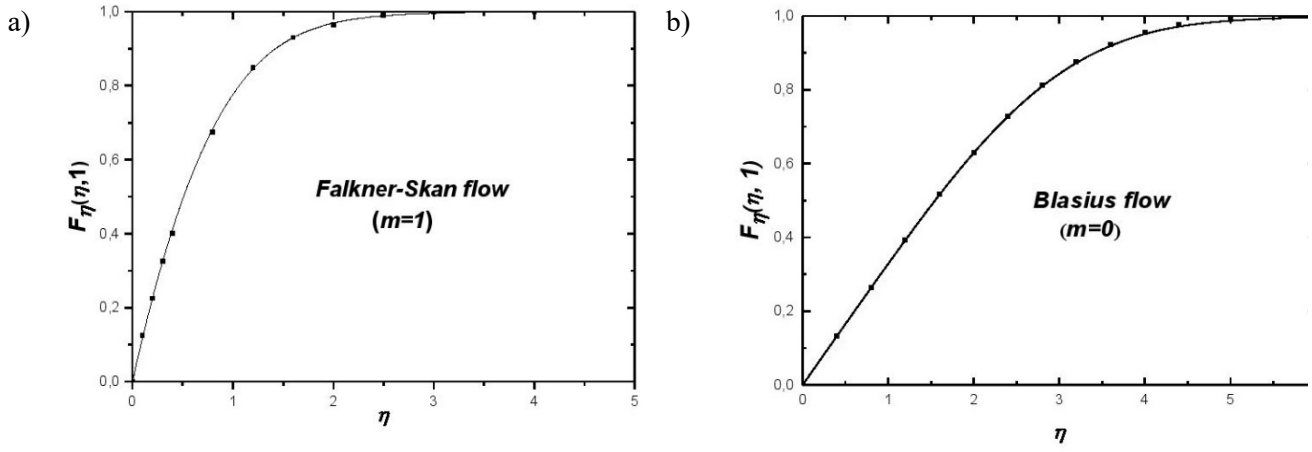

Fig.3. Dimensionless velocity profile for a) Blasius flow and b) Falkner-Skan flow: scatter points numerical results; solid lines present analytic approach.

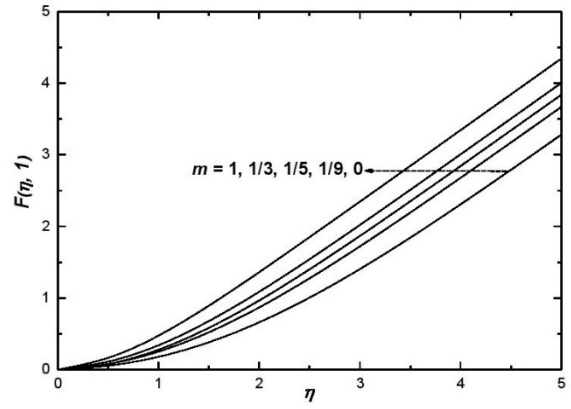

Fig. 4. Dimensionless stream function evolutions for five wedge surface directions.

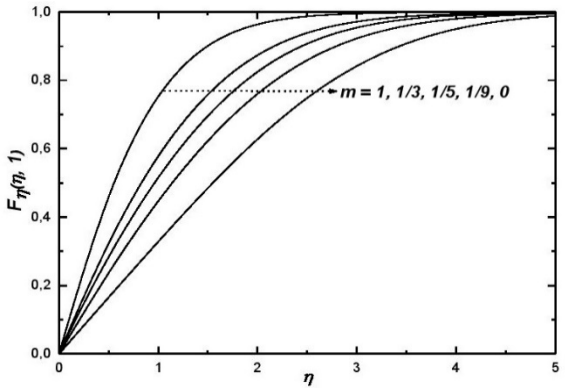

Fig.5. Dimensionless velocity profile distributions for five wedge surface directions.

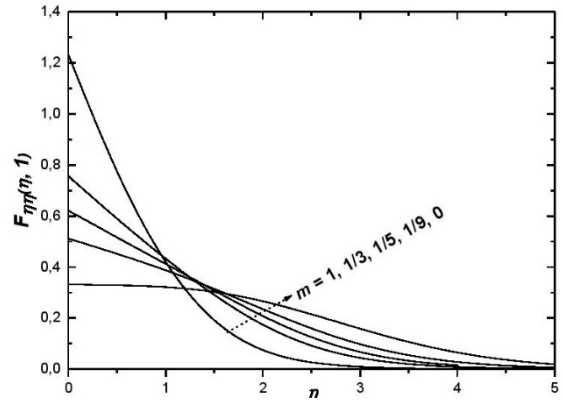

Fig.6. Variation of dimensionless local shear for five wedge surface directions.

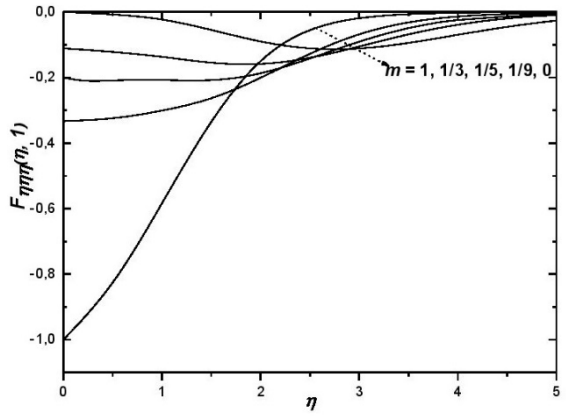

Fig.7. Variation of $F_{\eta\eta\eta}(\eta,1)$ for five wedge surface directions.

3.3. Case of all Strouhal numbers

In order to study analytically the unsteady boundary layer evolution for all Strouhal numbers, an ad hoc analytic expression of the dimensionless velocity profile $F_\eta(\eta,\xi)$ is proposed. This formula is the superposition of initial exact solution and steady approach solution with a minor perturbation of these solutions. The potency of this approach will be confirmed by the calculation of the mean residual error $\Delta\varepsilon$ of the below equation for all time values $0 \le \xi \le 1$ in the whole spacial domain $0 \le \eta < \eta_\infty$.

$$\frac{\partial^3 F}{\partial\eta^3}+\frac{1}{2}\eta(1-\xi)\frac{\partial^2 F}{\partial\eta^2}+\frac{1}{2}\Big[(m+1)\xi-(m-1)(1-\xi)\ln(1-\xi)\Big]F\frac{\partial^2 F}{\partial\eta^2}+$$
$$-(m-1)\left[\xi(1-\xi)\ln(1-\xi)\frac{\partial F}{\partial\xi}\right]\frac{\partial^2 F}{\partial\eta^2}+ \qquad (3.17)$$
$$+m\xi\left[1-\left(\frac{\partial F}{\partial\eta}\right)^2\right]+\xi(1-\xi)\left[1-(m-1)\ln(1-\xi)\frac{\partial F}{\partial\eta}\right]\frac{\partial}{\partial\xi}\left(\frac{\partial F}{\partial\eta}\right)=\Delta\varepsilon.$$

Under the above conditions, we express the velocity profile of the unsteady problem as the superposition of both the initial and steady solutions with a minor perturbation

$$F_\eta(\eta,\xi)=(1-\xi)\Big[erf\left(\eta\phi(\xi)\right)\Big]+\xi F_\eta(\eta,1) \qquad (3.18)$$

where $\phi(\xi)$ is a function depending on the wedge surface directions. Equation (3.18) verifies the boundary conditions and the two limits solutions as follows:

$$F_\eta(0,\xi)=F\ (0,\xi)=0,$$
$$F_\eta(\infty,\xi)=1,$$

at $\xi=0\ (St_x>>1)$, we find the initial solution of Rayleigh $F_\eta(\eta,0)=erf\left(\frac{1}{2}\eta\right)$, with $\phi(0)=\frac{1}{2}$ and at $\xi=1\ (St_x<<1)$, we find the steady approach solution Eq.(3.4) of Falkner-Skan equation.

The function $\phi(\xi) = \gamma_0 \xi + \frac{1}{2}$ verifies the two limits solutions and the determination of γ_0 constant can be found by the substitution of $F_\eta(\eta,\xi)$ in the momentum equation in which $\Delta\varepsilon$ must approach zero. Indeed, the results indicate that the dimensionless velocity profile corroborate well the equilibrium of the momentum equation for each wedge surface directions, with the maximum averaged residual errors $\Delta\varepsilon < 0.007$ for all Strouhal numbers in the whole domain of $\eta \in [0, \eta_\infty = 5]$. Therefore, the simplicity of terms existing in $F_\eta(\eta,\xi)$ converges well with the complexity of the unsteady momentum equation of the boundary layer flows over the wedge surface for all Strouhal numbers and for different wedge surface directions. An important physical function $F_{\eta\eta}(0,\xi)$ (shear stress) is given after derivation of Eq.(3.18),

$$F_{\eta\eta}(0,\xi) = \left.\frac{dF_\eta(\eta,\xi)}{d\eta}\right|_{\eta=0} = \frac{2}{\sqrt{\pi}}(1-\xi)\left(\gamma_0\xi + \frac{1}{2}\right) + \xi F_{\eta\eta}(0,1) \tag{3.19}$$

The local shear stress $F_{\eta\eta}(0,1)$ and γ_0 depend on the position of the wedge surface. Table 2 gives the values of γ_0 for different positions of the wedge surface.

Table 2. Values of γ_0 for different wedge surface positions.

m	*0*	*1/9*	*1/5*	*1/3*	*1*
$F_{\eta\eta}(0,1)$	*0.3320*	*0.5120*	*0.6213*	*0.7570*	*1.2326*
γ_0	*0.10*	*-0.08*	*-0.10*	*-0.12*	*0.06*

Figure 8 shows that the local shear stress determined from Eq.(3.19) is in a good accord with the of Williams-Rhyne numerical results for all-time values $0 \le \xi \le 1$. Therefore, the present approach confirms, in all spatial and temporal domains, the Rayleigh's, Blasius', Falknar-Skan's solutions and the general solution. Figure 9 presents the proposed velocity profile variation for different Strouhal number values in the spatial domain of $\eta \in [0, \eta_\infty \approx 5]$ and for different wedge surface directions. It is observed that for all Strouhal numbers, the velocity gradients are rapid when the wedge tends towards the vertical direction.

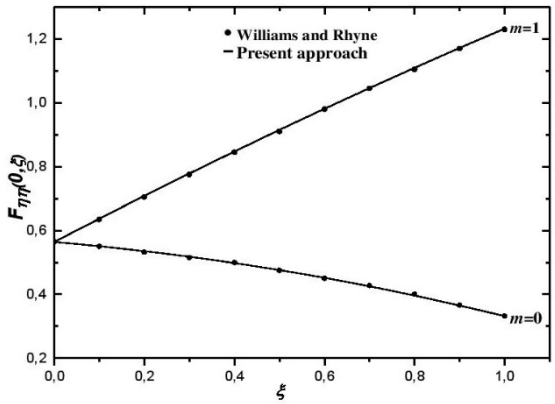

Fig.8. Local shear stress $F_{\eta\eta}(0,\xi)$ for vertical and horizontal wedge surface.

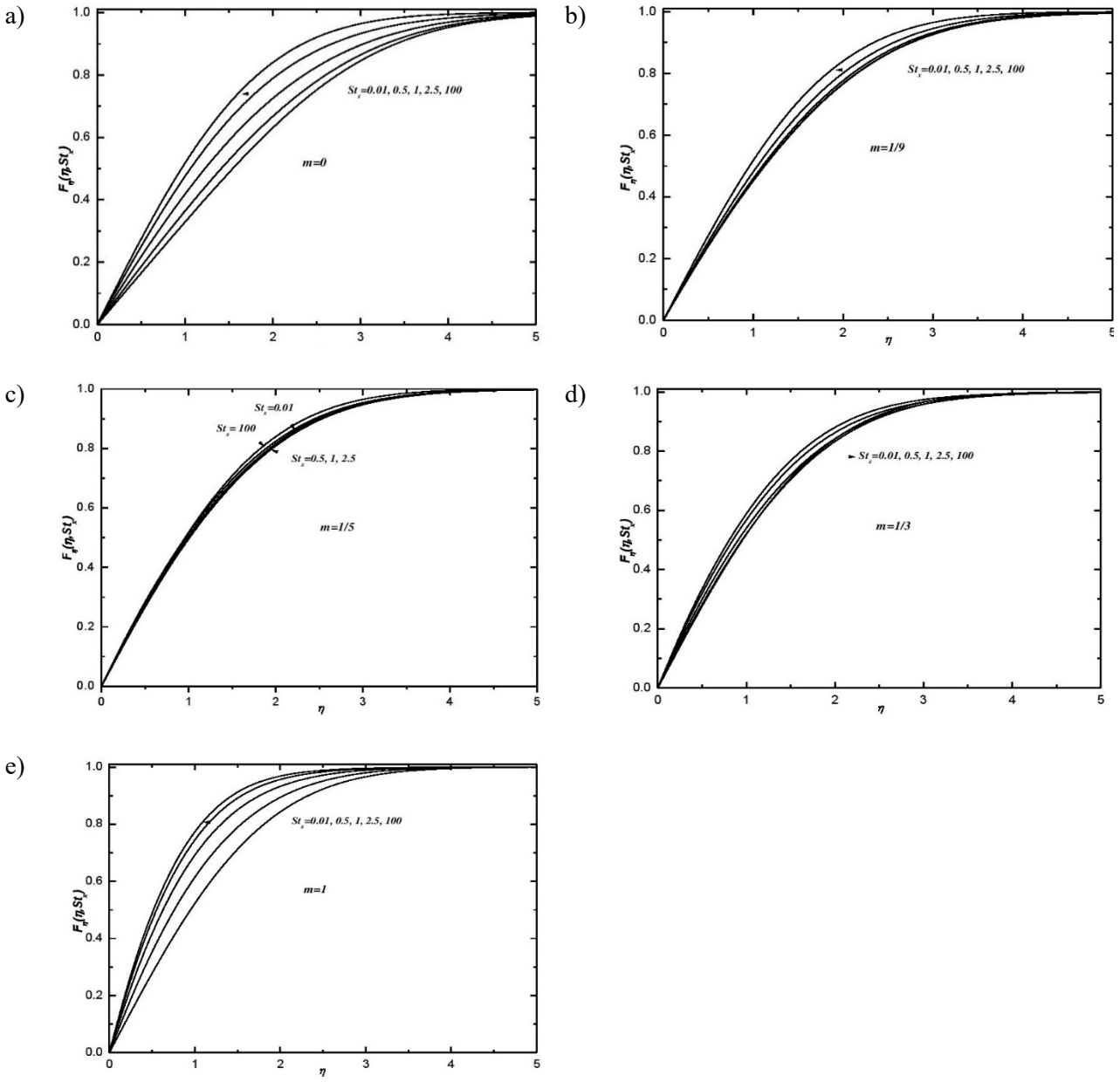

Fig.9. Dimensionless velocity profiles for all Strouhal numbers and for different wedge surface directions: a) $m=0$, b) $m=1/9$, c) $m=1/5$, d) $m=1/3$, e) $m=1$.

These results are well explained in Figs 10-11. Furthermore, when the wedge surfaces are horizontal or vertical, the curves of the velocity evolutions are clearly separated for each St number value. However, in case of inclination positions of the wedge surface the velocity evolutions are identical when $St>1$ and with a light variation when $St<1$.

The skin friction coefficient on the surface can be expressed as:

$$C_f = 2\mu\left(\frac{\partial u}{\partial y}\right)_{y=0}\frac{1}{\rho u_e{}^2}.$$

Using similarity solution, we find

$$\frac{C_f}{\mathrm{Re}_x^{-1/2}} = 2\xi^{-1/2}\left[\frac{2}{\sqrt{\pi}}(1-\xi)\left(\gamma_0\xi+\frac{1}{2}\right)+\xi F_{\eta\eta}(0,1)\right]. \tag{3.20}$$

To show the effect of the Strouhal number on the evolutions of the main physical parameters, the local shear stress and the skin friction coefficient are illustrated in Figs 10-11 for all Strouhal number values and for different wedge directions. Indeed, when $St_x < 1$, the variations of the skin friction coefficient are more significant for the horizontal surface ($m=0$) and becomes lightly less important for inclined and vertical positions of the wedge. On the other hand, when $St_x > 1$ the evolutions of the skin friction coefficient depending linearly on the Strouhal number and become equal for all $St_x > 80$. We explain this results by the fact that when $St_x > 1$ ($\delta_c > \delta_d$) the diffusion forces dominate, and when $St_x < 1$ ($\delta_d > \delta_c$) the convective forces dominate.

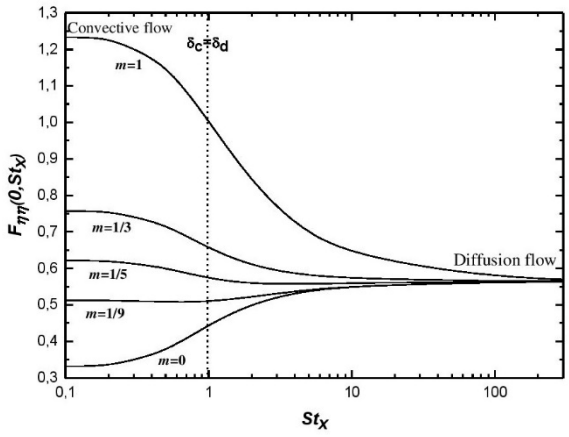

Fig.10. Local shear stress evolutions for all Strouhal numbers and for different wedge surface directions.

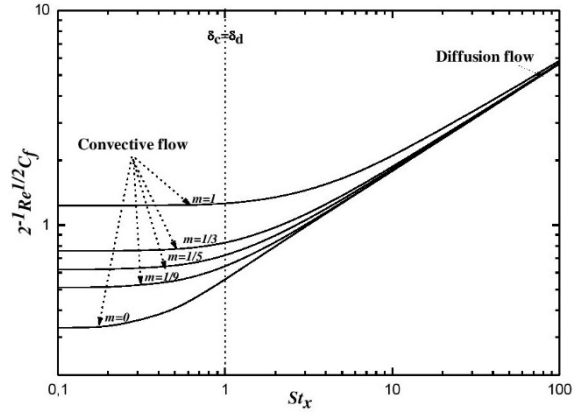

Fig.11. Skin friction coefficient for all Strouhal numbers and for different wedge surface directions.

4. Conclusion

An analytic approach is employed to study an unsteady boundary layer flow along a wedge surface for all Strouhal numbers. An analytical formula of the velocity profile is proposed for converging the momentum equation at any wedge surface directions and for all time values. This approach has been well verified the

boundary conditions, Rhyleigh's, Blasius', Falknar-Skan's and Williams-Rhyne's solutions and the unsteady momentum equation for all Strouhal numbers and for all spatial and temporal domains. A new analytic law of the skin friction coefficient is given for all Strouhal numbers and at any wedge surface directions $0 \leq m \leq 1$. It is clear that the simplicity of terms existing in the velocity formula converges well with the complexity of nonlinear partial differential equation of the unsteady boundary layer developed over the wedge surface.

Acknowledgements

The authors thank the management of Matter Sciences Department, Faculty of Sciences -University of Amar Telidji for their continuous support to carry out this research work.

Nomenclature

A, B, C – constants
C_f – skin friction coefficient
F – dimensionless stream function
F_η – dimensionless velocity profile
m – Falkner-Skan parameter
Re – Reynolds number
St – Strouhal number
t – time, s
u_e – ambient velocity, $m.s^{-1}$
u – velocity component in the x-direction, $m.s^{-1}$
ν – velocity component in the y-direction, $m.s^{-1}$
x, y – Cartesian coordinates along the wedge surface and normal to it, respectively, m

Greek symbols

α_0,β_0,γ_0 – constants
δ_c – convective flow thickness, m
δ_d – diffusion flow thickness, m
$\Delta\varepsilon$ – average residual error
η – independent similarity variable
μ – dynamic viscosity, $kg.\ m^{-1}.s^{-1}$
ν – kinematic viscosity, $m^2.\ s^{-1}$
ξ – independent similarity variable
$\pi\beta$ – wedge surface angle, *rad*
ρ – density, $kg.m^{-3}$
σ – function
ϕ – function depending on ξ
ψ – stream function, $m^2.s^{-1}$

Subscripts

η – differentiation with respect to η
max – maximum

References

[1] Stewartson K. (1951): *On the impulsive motion of a flat plate in a viscous fluid (Part I)*.– Quart. J. Mec. App. Math., vol.4, pp.182-198. https://doi.org/10.1093/qjmam/4.2.182.

[2] Stewartson K. (1973): *On the impulsive motion of a flat plate in a viscous fluid (Part II)*.– Quart. J. Mec. App. Math., vol. 22, pp.143-152, https:// doi :10.1093/QJMAM/26.2.143.

[3] Tokuda N. (1968): *On the impulsive motion of a flat plate in a viscous fluid*.– J. Fluid Mec., vol.33, pp.657-675, doi: 10.1017/S0022112068001606.

[4] Watkins C.B.(1975): *Heat transfer in the boundary layer over an impulsively started flat plate*.– ASME, J. Heat Trans., vol.97, No.3, pp.482-484, 1975ATJHT..97..482W.

[5] Hall M.G. (1969): *The boundary layer over an impulsively started flat plate*.– Proc. Royal Soc. Lon. A, vol.310, pp.401-414, https://www.jstor.org/stable/2416386.

[6] Dennis S.C.R. (1972): *The motion of a viscous fluid past an impulsively started semi-infinite flat plate*.– J. App. Math, vol.10, No.1, pp.105-107, https://doi.org/10.1093/imamat/10.1.105.

[7] Seshadri R., Sreeshylan N. and Nath G. (2002): *Unsteady mixed convection flow in the stagnation region of a heated vertical plate due to impulsive motion*.– Int. J. Heat and Mass Trans., vol.45, No.6, pp.1345-1352, https://doi.org/10.1016/S0017-9310(01)00228-9.

[8] Williams J.C. and Rhyne T.H.(1980): *Boundary layer development on a wedge impulsively set into motion*.– SIAM, J. App. Math., vol.38, No.2, pp.215-124, https://doi.org/10.1137/0138019.

[9] Nazar N., Amin N. and Pop, I.(2004): *Unsteady boundary layer flow due to stretching surface in a rotating fluid*.– Mec. Res. Commu., vol.31, No.1, pp.121-128, https://doi.org/10.1016/j.mechrescom.2003.09.004.

[10] Sajid M., Ahmad I., Hayat T. and Ayub M. (2009): *Unsteady flow and heat transfer of a second grade fluid over a stretching sheet*.– Commun. Nonl. Sci. Num. Simul., vol.14, No.1, pp.96-108, https://doi.org/10.1016/j.cnsns.2007.07.014.

[11] Liao S.J. (2004): *On the homotopy analysis method for nonlinear problems*.– Appl. Math. Comput., vol.147, No.2, pp.499-513, https://doi.org/10.1016/S0096-3003(02)00790-7.

[12] Liao S. J. (2006): *An analytic solution of unsteady boundary-layer flows caused by an impulsively stretching plate*.– Commun. Nonlin. Sci. Num. Simul., vol.11, No.3, pp.326-339, https://doi.org/10.1016/j.cnsns.2004.09.004.

[13] Hang X. Liao, S.J. and Ioan P. (2007): *Series solutions of unsteady three-dimensional MHD flow and heat transfer in the boundary layer over an impulsively stretching plate*.– Europ. J. Mec. B / Fluids, vol.26, No.1, pp.15-27. https://doi.org/10.1016/j.euromechflu.2005.12.003.

[14] Hang X., Liao, S. J. and Ioan P. (2008): *Series solutions of unsteady free convection flow in the stagnation-point region of a three-dimensional body*.– Int. J. Therm. Sci., vol.47, No.5, pp. 600-608, https://doi.org/10.1016/j.ijthermalsci.2007.05.001.

[15] Howarth L. (1938): *On the solution of the laminar boundary layer equations*.– Proc. Royal Soc. Lon. A, vol.164, pp.547-579, https://doi.org/10.1098/rspa.1938.0037.

[16] Bachiri M. and Bouabdallah A. (2011): *Analytical approach of unsteady boundary-layer flow over a semi-infinite plate for all Strouhal numbers*.– ASME, J. Appl. Mec., vol.78, No.2., pp.1-5, https://doi.org/10.1115/1.4002571.

[17] Bachiri M. and Bouabdallah A. (2012): *Analytical study of the convection heat transfer from an isothermal wedge surface to fluids*.– ASME, J. Heat Trans., vol.134, No.6., pp.1-5, https://doi.org/10.1115/1.4006030.

[18] Zheng Z.C. and Ghate A.S. (2015): *A solution of two-parameter asymptotic expansions for a two-dimensional unsteady boundary layer*.– Appl. Math. Comput., vol.270, No.1, pp.90-104, https://doi.org/10.1016/j.amc.2015.08.016.

[19] Hafidzuddin M.E.H., Roslinda N., Norihan M.A. and Ioan P. (2018): *Unsteady flow and heat transfer over a permeable stretching/shrinking sheet with generalized slip velocity*.– Int. J. Num. Metho. for Heat and Fluid Flow., vol.28, No.6, pp.1457-1470, https://doi.org/10.1108/HFF-11-2016-0440.

[20] Nagler J. (2019): *Higher order solution of Boundary layer formation as a result of impulsive start of motion*.– ZAMM, J. Appl. Math. Mech., vol.99, No.3., pp.1-7, https://doi.org/10.1002/zamm.201800124.

[21] Bulgakov V.N., Kotenev V.P. and Ozhgibisova l. (2020): *Analytical study of laminar boundary layer near blunted Bodies*.– Math. Mod. Comp. Simul., vol.12, pp.60-69, https://doi.org/10.1134/S0234087919060054.

Received: January 24, 2022
Revised: November 15, 2022